

Highly reproducible superconductivity in potassium-doped triphenylbismuth

Ren-Shu Wang,^{1,2} Jia Cheng,¹ Xiao-Lin Wu,¹ Hui Yang,¹ Xiao-Jia Chen,^{2,*} Yun Gao,^{1,†} and Zhong-Bing Huang^{1,‡}

¹*School of Materials Science and Engineering, Faculty of Physics and Electronic Technology, Hubei University, Wuhan 430062, China*

²*Center for High Pressure Science and Technology Advanced Research, Shanghai 201203, China*

(Dated: April 18, 2022)

Using a new two-step synthesis method - ultrasound treatment and low temperature annealing, we explore superconductivity in potassium-doped triphenylbismuth, which is composed of one bismuth atom and three phenyl rings. The combination of dc and ac magnetic measurements reveals that one hundred percent of synthesized samples exhibit superconductivity at 3.5 K and/or 7.2 K at ambient pressure. The magnetization hysteresis loops provide a strong evidence of type-II superconductor, with the upper critical magnetic field up to 1.0 Tesla. Both calculated electronic structure and measured Raman spectra indicate that superconductivity is realized by transferring electron from potassium to carbon atom. Our study opens an encouraging window for the search of organic superconductors in organometallic molecules.

PACS number(s):74.70.Kn, 74.25.-q, 78.30.Jw

Introduction— Superconductivity in organic materials has been attracting great attention due to its fundamental importance and potential application prospect. Following the discovery of superconductivity in (TMTSF)₂PF₆ in 1980 [1], several organic superconducting (SC) families have been reported including charge transfer complexes [2], fullerides [3], and graphites [4, 5]. In 2010, potassium doped picene was shown to display a SC transition temperature T_c as high as 18 K [6], which provides a platform to explore superconductivity in organic hydrocarbons. Soon thereafter, potassium doped phenanthrene [7] and dibenzopentacene [8] were found to exhibit superconductivity at 5 K and 33 K, respectively. The above three molecules belong to fused hydrocarbons, in which five, three, and seven phenyl rings are fused via sharing sides. Very recently, we found that by doping potassium into *p*-terphenyl, a hydrocarbon formed by connecting three phenyl rings with C-C bond, SC transitions can be observed at 123 K, 43 K, and 7.2 K [9]. The observation of distinct T_c in these hydrocarbons suggests that both the number and connecting pattern of phenyl rings play important roles in the SC property.

Despite tremendous efforts by the scientific community [10–15], the detailed crystal structures of hydrocarbon superconductors have not yet been determined in experiments so far, due to low reproducibility of SC samples and vanishingly small SC fraction. This places a serious restriction on deep understanding of their physical properties. To make progress on hydrocarbon superconductors, we develop a two-step synthesis method - ultrasound treatment and low temperature annealing to explore superconductivity in potassium-doped triphenylbismuth. As a member of organometallic molecules [16], triphenylbismuth has been used as the solidifying catalyst for butyl hydroxyl propellant of high combustion velocity, as well as the catalyst for some monomers' polymerization [17]. In each triphenylbismuth molecule, three phenyl rings and one bismuth atom are connected by single C-Bi bond. Such an arrangement of phenyl rings is distinct from the ones in fullerides [3], graphites [4, 5], fused hydrocarbons [6–8], and *p*-terphenyl [9]. In view of these facts, exploration of superconductivity in potassium-doped triphenylbismuth not only

enriches the functionalities of organometallic compounds but also provides a new platform for understanding the relationship between SC property and molecular structure.

Potassium-doped triphenylbismuth was synthesized by the following steps. High-purity potassium metal (99% purity, Sinopharm Chemical Reagent) was cut into small pieces and mixed with triphenylbismuth (>98% purity, Tokyo Chemical Industry) with a mole ratio of $x : 1$ ($x=1, 2, 2.5, 3$ and 3.5). The mixtures were then loaded into quartz tubes and sealed under high vacuum (1×10^{-4} Pa). The sample tubes were treated in an ultrasound device at 90 °C for 10 hours. After ultrasound treatment, the samples tubes were heated at 130 °C for 1-5 days. Here, ultrasound treatment was adopted to mix potassium and triphenylbismuth thoroughly, and low temperature annealing can avoid producing KH via reaction of potassium and hydrogen, which is crucial for crystallization of doped materials. For each run of experiment, the sample from the same tube was distributed into several nonmagnetic capsules and sealed by GE varnish in a glove box with the oxygen and moisture levels less than 0.1 ppm.

Magnetic property of potassium-doped triphenylbismuth— Superconductivity was revealed by both the dc and ac magnetic measurements performed on our samples with a SQUID magnetometer (Quantum Design MPMS3). Pristine triphenylbismuth exhibits a weak diamagnetic behavior, which is clearly characterized by the small negative magnetic susceptibility in the temperature range of 1.8-300 K. Upon doping potassium into triphenylbismuth, all synthesized samples listed in Table I exhibit a SC transition temperature of ~ 3.5 K, and four samples also show a transition at 7.2 K. The representative results for samples D ($x=3$, annealed for 3 days) and E ($x=2$, annealed for 5 days) are summarized in Fig. 1. Figure 1a shows the dc magnetic susceptibility χ for sample D in the applied magnetic field of 10 Oe with field cooling (FC) and zero-field cooling (ZFC) in the temperature range of 1.8-11 K. Both FC and ZFC susceptibilities show a sudden decrease around 3.5 K. Such a sudden drop of χ is consistent with the well-defined Meissner effect, supporting the occurrence of superconductivity in sample D. The shielding volume fraction at 1.8 K is estimated to be about 1.7%, and larger val-

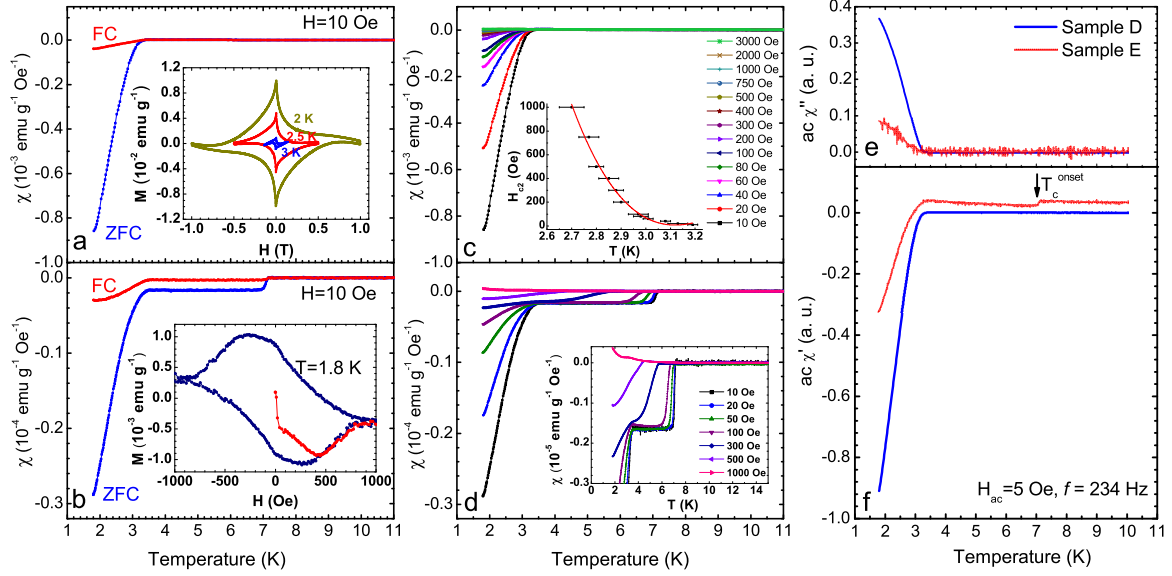


FIG. 1. (Color online) **a, b**, The temperature dependence of the dc magnetic susceptibility χ for samples D and E in the applied magnetic field of 10 Oe with field cooling (FC) and zero-field cooling (ZFC). The inset figures show the magnetization loops of samples D and E, with measured temperature shown beside the corresponding loop. **c, d**, The temperature dependence of χ for samples D and E measured at various magnetic fields in the ZFC run. The inset figure in **c** shows the upper critical magnetic field H_{c2} in the temperature region of 2.7-3.2 K. The inset figure in **d** displays the transition around 7.2 K with enlarged scale. **e, f**, Imaginary χ'' and real χ' components of the ac magnetic susceptibility as a function of temperature. The probe harmonic magnetic field and frequency are 5 Oe and 234 Hz, respectively.

TABLE I. List of K_x triphenylbismuth samples synthesized in this study. Both T_c^{onset} and T_c were read out from the ZFC run measured in the applied magnetic field of 10 Oe. The former denotes the temperature where the magnetic susceptibility turns to suddenly decrease with lowering the temperature, and the latter is determined from the intercept of linear extrapolations from below and above T_c^{onset} .

Sample label	x	Annealing time (days)	T_c^{onset}	T_c
A	3	1	3.39	3.19
B	1	3	3.06	2.90
C	2	3	3.56 & 7.28	3.35 & 7.19
D	3	3	3.49	3.32
E	2	5	3.51 & 7.18	3.29 & 7.13
F	2.5	5	3.46	3.30
G	3	5	3.52 & 7.17	3.32 & 7.06
H	3.5	5	3.53 & 7.25	3.28 & 7.13

ues are expected with further lowering the temperature since χ does not saturate at 1.8 K. Similarly, sudden drops of χ around 3.5 and 7.2 K indicate that there exist two SC phases in sample E (Fig. 1b). Notice that the drop at 7.2 K is much weaker than the one at 3.5 K, implying that sample E is dominated by the SC phase with $T_c \sim 3.5$ K.

The inset of Fig. 1a shows the magnetization loops of sample D with magnetic field up to 1.0 T measured at 2, 2.5, and 3 K in the SC state. The hysteresis loops along the two op-

posite magnetic field directions show a clear diamond-like shape, providing a strong evidence for the type-II superconductor. One can readily see that the dip or peak of the magnetization loops appears at magnetic field close to 0 T, indicating a very small lower critical magnetic field H_{c1} for the SC phase at 3.5 K. The expansion of the diamond from 3 K to 2 K reflects the fact that the upper critical magnetic field H_{c2} increases with lowering the temperature. The type-II SC behavior is also applied for sample E, as seen from the magnetization loop with magnetic field up to 1000 Oe measured at 1.8 K in the inset of Fig. 1b. One significant difference from the magnetization loops of sample D is that the diamond shape is strongly distorted, due to the coexistence of two SC phases in sample E.

The obtained superconductivity in potassium-doped triphenylbismuth was also supported by the evolution of the χ -T curve with the applied magnetic fields (Fig. 1c, Fig. 1d and the inset of Fig. 1d). The χ -T curve gradually shifts towards the lower temperatures with increasing magnetic field. This character is consistent with the intrinsic property of a superconductor, i.e., the SC transition temperature T_c is gradually decreased with increasing magnetic field. In the inset of Fig. 1c, we show the temperature dependence of the upper critical magnetic field H_{c2} for sample D in the temperature region of 2.7-3.2 K. Here, H_{c2} is determined from the χ -T curves measured at various magnetic fields. A dramatic increase of

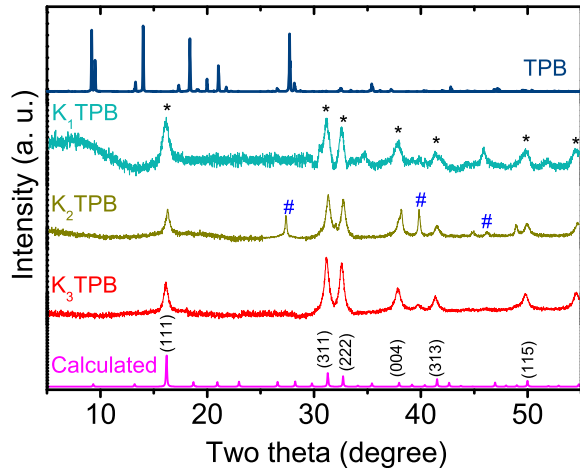


FIG. 2. (Color online) XRD patterns of pristine and potassium-doped triphenylbismuth measured at room temperature. In figures 2 and 5, TPB, K_1 TPB, K_2 TPB, and K_3 TPB correspond to pristine triphenylbismuth, samples B, E, and D, respectively. The symbol * represents the common XRD pattern for the three samples, and the symbol # stands for the solitary XRD pattern for sample E. The purple curve at the bottom represents the calculated XRD pattern of optimized structure in Fig. 3b.

H_{c2} with lowering the temperature is clearly evidenced in the investigated temperature region.

The ac magnetic susceptibility measurements were adopted to make a further confirmation for the observed superconductivity. This technique has been successfully used to study numerous superconductors including high- T_c cuprates [18], heavy-fermion material $CeCu_2Si_2$ [19], and iron-based $FeSe_{1-x}$ [20]. The real component χ' of the ac susceptibility is a measure of the magnetic shielding and the imaginary component χ'' reflects the magnetic irreversibility [18]. Figures 1e and 1f present the temperature dependence of χ'' and χ' of the ZFC ac susceptibility, respectively. For sample D (blue lines), two inflection anomalies occur in the χ'' -T and χ' -T curves upon cooling at the exactly same temperature of 3.5 K, which coincides with the T_c value already determined from Fig. 1a. As can be seen, both χ' and χ'' are close to zero above the transition due to the absence of flux exclusion in the normal state. Upon entering the SC state below 3.5 K, the diamagnetic behavior leads to a negative χ' which becomes more negative as more flux is expelled from the sample with lowering the temperature. Here, a finite χ'' reflects the fact that the flux penetrating the sample lags the external flux. Similar inflection anomalies are also observed for sample E (red lines) around 3.5 K. However, only χ' exhibits an anomaly for the SC transition at 7.2 K and no visible change can be found for χ'' . This is attributed to the small fraction of the 7.2 K SC phase.

Crystal structures of pristine and potassium-doped triphenylbismuth— X-ray diffraction (XRD) spectrometer

(Panalytical Emperean) was employed to examine the evolution of the crystal structure from pristine to potassium-doped triphenylbismuth. Figure 2 displays the XRD patterns of pristine and potassium-doped samples with mole ratio $x=1, 2,$ and 3 . The peak positions for the pristine material are in good agreement with the ones in the standard PDF card. Pristine triphenylbismuth is a typical kind of molecular solid and crystallizes in the space group $C2/c$ (No. 15), with eight molecules of $C_{18}H_{15}Bi$ in a unit cell of dimensions $a=27.70 \text{ \AA}$, $b=5.82 \text{ \AA}$, $c=20.45 \text{ \AA}$, and $\beta=114.48^\circ$ [21, 22], as shown in Fig. 3a. The mean Bi-C distance is 2.24 \AA and the mean C-Bi-C bond angle is about 94° . Upon doping potassium, no obvious peak appears at the positions where the pristine material shows strong peaks and the XRD feature is completely different from the undoped case. This indicates that doping of potassium atoms produces a new crystal structure.

Notice that the samples with different x 's exhibit a common XRD pattern marked by *, while the sample with $x=2$ also shows a solitary pattern marked by #, which is actually consistent with the XRD pattern of metal Bi. The existence of Bi in sample E is evidenced by the appearance of colorless and transparent liquid on the inner wall of tube, indicating that partial triphenylbismuth molecules are decomposed into Bi atoms and phenyls. Given that all the three samples exhibit superconductivity around 3.5 K, it is reasonable to ascribe the 3.5 K SC phase to the crystal structure represented by *. As to the 7.2 K SC phase observed in sample E, its very small fraction makes it hard to discern the corresponding crystallization information from the XRD results.

To identify the complicated crystal structure for the 3.5 K SC phase, we first employed the Universal Structure Predictor: Evolutionary Xtallography (USPEX) based on the genetic algorithm [23] to search for global stable or metastable structures in the phase diagram of K_yBi with $y=1-4$, which correspond to the possible arrangement of potassium and bismuth atoms in the doped materials. In the search process, the plane-wave pseudopotential method as implemented in the Vienna *ab initio* simulation package (VASP) program [24, 25] was adopted to relax the atomic positions. The generalized gradient approximation (GGA) with Perdew-Burke-Ernzerhof (PBE) formula [26] for the exchange-correlation potentials and the projector-augmented wave method (PAW) [27] for ionic potential were used to model the electron-electron and electron-ion interactions. The searched results indicate that one cubic structure of K_4Bi could reflect the main character of measured XRD pattern. Then we replace bismuth atom with triphenylbismuth in this structure and perform a full relaxation of atomic positions. The optimized crystal has three molecules of $C_{18}H_{15}Bi$ and twelve K atoms in a unit cell of dimensions $a=b=c=9.473 \text{ \AA}$, and $\alpha = \beta = \gamma = 90^\circ$, as shown in Fig. 3b. Potassium atoms represented by blue balls in Fig. 3b are intercalated in the interstitial space of bismuth and phenyl rings, with deep blue one close to a certain phenyl ring and light blue one occupying the center of green dashed line connecting two bismuth atoms. The powder XRD pattern based

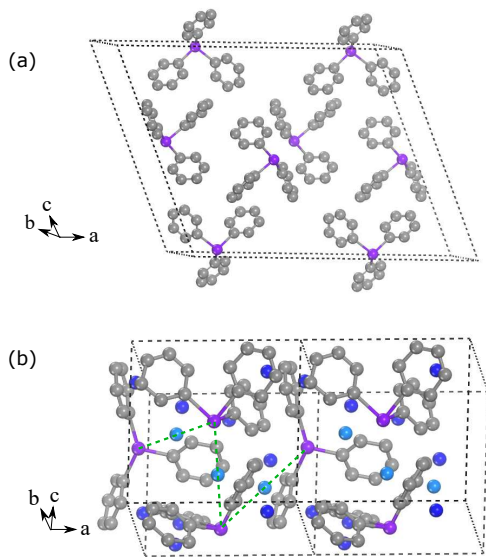


FIG. 3. (Color online) (a) The molecular arrangement in pristine triphenylbismuth is shown in a single cell; (b) The arrangement of molecules and potassium in doped material is shown in a $2 \times 1 \times 1$ supercell. The grey, purple, and blue balls represent carbon, bismuth, and potassium atoms, respectively. The hydrogen atoms are not given in the figure for clarity.

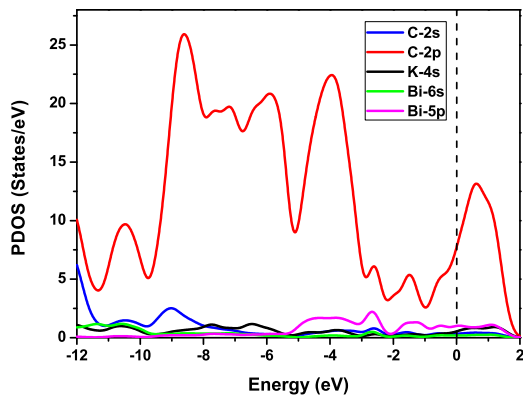


FIG. 4. (Color online) Orbital-resolved partial density of states (PDOS) as a function of energy. The Fermi energy is set to be zero. The red, blue, black, green, and purple solid lines represent PDOS of C-2p, C-2s, K-4s, Bi-6s, and Bi-5p orbitals, respectively.

on the optimized crystal, shown at the bottom of Fig. 2, is in good agreement with the one marked by *. This indicates that the doped materials crystallize into the optimized cubic structure with high probability. The missing of weak peaks in K_x TPB ($x=1-3$) compared with the theoretical modeling is mostly possible due to poor crystallization, manifested by broad XRD peaks in Fig. 2.

The orbital-resolved partial density of states (PDOS) for the optimized crystal are presented in Fig. 4. The existence of fi-

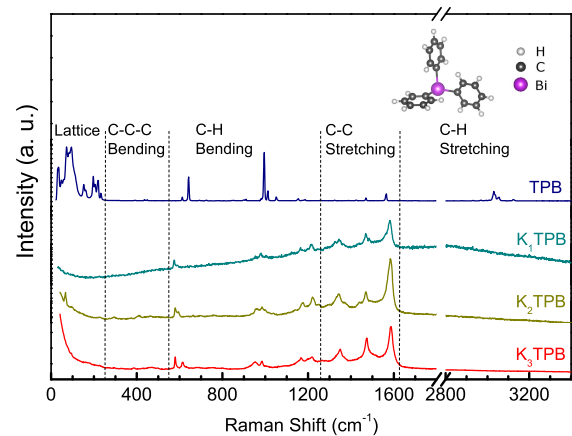


FIG. 5. (Color online) Raman scattering spectra of pristine and potassium-doped triphenylbismuth collected at room temperature. Upper right presents the molecular structure of triphenylbismuth. Five regions of Raman active modes, divided by the vertical dashed lines, are shown above the spectra of pristine material.

nite PDOS at the Fermi energy indicates that the potassium-doped system actually lies in the metallic state, providing a support for the observation of superconductivity at 3.5 K. Among the five orbital shown in Fig. 4, the C-2p orbital makes a dominant contribution to PDOS in the vicinity of the Fermi energy, while the K-4s orbital has little contribution. This result reflects the fact that the electron is transferred from K-4s to C-2p, which not only leads to the metallic behavior but also strongly affects the vibrations of phenyl rings.

Raman spectra of pristine and potassium-doped triphenylbismuth— The SC phase was further characterized by phase-sensitive Raman spectra, which were collected on an in-house system with Charge Coupled Device and Spectrometer from Princeton Instruments. Five regions of Raman active modes from the low to high frequencies correspond to the lattice and Bi-phenyl, C-C-C bending, C-H bending, C-C stretching, and C-H stretching modes [28]. We observed all these modes in pristine triphenylbismuth. Upon doping potassium into triphenylbismuth, all lattice modes are dramatically suppressed and the modes in the C-H stretching region become invisible (see Figure 5).

Significant differences of the spectra between the pristine and doped samples are in the C-H bending and C-C stretching regions. Upon doping potassium, the 644 and 993 cm^{-1} C-H bending modes in the pristine material shift down with a dramatic decrease in the intensity. By contrast, the C-H bending modes at 1154 and 1182 cm^{-1} shift up with an increase in the intensity. It is obvious that the mode intensity in the whole C-C stretching region gets a strong enhancement in the doped samples. An upshift of Raman spectra is also observed for the two peaks at 1322 and 1564 cm^{-1} in the pristine material, while the peak at 1469 cm^{-1} does not shift its position with the potassium doping.

The observation of both red and blue shifts of Raman

spectra in potassium-doped triphenylbismuth is quite different from the situation in potassium-doped phenanthrene [7] and picene [10], where only red shifts were observed. Such red shifts were attributed to the softening of Raman modes by the transferred electrons from potassium to phenanthrene and picene molecules. This mechanism should also work for triphenylbismuth, making the Raman modes tend to shift down. On the other hand, when phenyl is connected to an X (either metal [29] or halogen [30]) atom, both the C-H and C-C modes are affected by the C-X bond. In the halogenobenzenes [30], the frequencies of the C-C stretching modes increase from I-benzene to F-benzene, suggesting that an increase of benzene polarization with increasing the electronegativity of halogen atom makes the Raman modes tend to shift up. Based on the above analyses, the Raman shifts in our samples could be understood as the competing results between transferred electrons and enhanced polarization of phenyls, which is clearly manifested by the asymmetric Raman line shape and the increase of Raman intensity in the C-C stretching region.

Conclusion—The present results provide unambiguous evidence for highly reproducible superconductivity in potassium-doped triphenylbismuth. The existence of 3.5 K and 7.2 K SC transitions indicates that two stable crystal structures can be formed upon doping potassium into triphenylbismuth. Similar SC transitions around 7.2 K were also observed in potassium-doped picene [6], dibenzopentacene [8], and *p*-terphenyl [9]. The insensitivity of T_c to the details of molecules suggests that the SC phase around 7.2 K rests mainly on the common structural unit - phenyl ring. On the other hand, the findings of SC phases with much higher T_c 's (18 K in picene [6], 33 K in dibenzopentacene [8], and above 120 K in *p*-terphenyl [9]) indicate that the arrangement of phenyl rings plays a crucial role in boosting superconductivity.

The unique feature of triphenylbismuth-like organometallic molecules is the presence of metal atom connecting phenyl rings. Since the structure of such systems depends sensitively on the metal atom, finding materials with different T_c 's is expected, which provides a bottom-up understanding of the SC mechanism in the phenyl-ring-based organic superconductors.

R.S.W. and J.C. contribute equally to this work. We thank Hai-Qing Lin for strong support and valuable discussion. This work was supported by the National Natural Science Foundation of China under Grants Nos. 11574076, 11674087, and 91221103.

* xjchen@hpstar.ac.cn

† gaoyun@hubu.edu.cn

‡ huangzb@hubu.edu.cn

[1] D. Jérôme, A. Mazaud, M. Ribault, and K. Bechgaard, *J. Phys. Lett.* **41**, L95-98 (1980).

- [2] T. Ishiguro, K. Yamaji, and G. Saito, *Organic Superconductors* (2nd edition, Springer-Verlag, 1997).
- [3] A. F. Hebard, M. J. Rosseinsky, R. C. Haddon, D. W. Murphy, S. H. Glarum, T. T. M. Palstra, A. P. Ramirez, and A. R. Kortan, *Nature* **350**, 600-601 (1991).
- [4] N. Emery, C. Hérold, M. d'Astuto, V. Garcia, Ch. Bellin, J. F. Mareche, P. Lagrange, and G. Louprias, *Phys. Rev. Lett.* **95**, 087003 (2005).
- [5] J. S. Kim, L. Boeri, J. R. O'Brien, F. S. Razavi, and R. K. Kremer, *Phys. Rev. Lett.* **99**, 027001 (2007).
- [6] R. Mitsuhashi, Y. Suzuki, Y. Yamanari, H. Mitamura, T. Kambe, N. Ikeda, H. Okamoto, A. Fujiwara, M. Yamaji, N. Kawasaki, Y. Maniwa, and Y. Kubozono, *Nature* **464**, 76-79 (2010).
- [7] X. F. Wang, R. H. Liu, Z. Gui, Y. L. Xie, Y. J. Yan, J. J. Ying, X. G. Luo, and X. H. Chen, *Nature Commun.* **2**, 507-513 (2011).
- [8] M. Xue, T. Cao, D. Wang, Y. Wu, H. Yang, X. Dong, J. He, F. Li, and G. F. Chen, *Sci. Rep.* **2**, 389 (2012).
- [9] R. S. Wang, Y. Gao, Z. B. Huang, and X. J. Chen, arXiv: 1703.06641, arXiv: 1703.05804, arXiv: 1703.05803 (2017).
- [10] T. Kambe, X. He, Y. Takahashi, Y. Yamanari, K. Teranishi, H. Mitamura, S. Shibusaki, K. Tomita, R. Eguchi, H. Goto, Y. Takabayashi, T. Kato, A. Fujiwara, T. Kariyado, H. Aoki, and Y. Kubozono, *Phys. Rev. B* **86**, 214507 (2012).
- [11] A. Ruff, M. Sing, R. Claessen, H. Lee, M. Tomić, H. O. Jeschke, and R. Valentí, *Phys. Rev. Lett.* **110**, 216403 (2013).
- [12] S. Heguri, Q. Thi Nhu Phan, Y. Tanabe, and K. Tanigaki, *Phys. Rev. B* **90**, 134519 (2014).
- [13] G. A. Artioli, F. Hammerath, M. C. Mozzati, P. Carretta, F. Corana, B. Mannucci, S. Margadonna, and L. Malavasi, *Chem. Commun.* **51**, 1092 (2015).
- [14] S. Heguri, M. Kobayashi, and K. Tanigaki, *Phys. Rev. B* **92**, 014502 (2015).
- [15] Y. Gao, R. S. Wang, X. L. Wu, J. Cheng, T. G. Deng, X. W. Yan, and Z. B. Huang, *Act. Phys. Sin.* **65**, 077402 (2016).
- [16] C. Elschenbroich, *Organometallics* (3rd edition, Weinheim: Wiley-VCH-Verl., 2006).
- [17] M. Dötterl and H. G. Alt, *Chemcatchem* **4**, 370-378 (2012).
- [18] F. Gömör, *Supercond. Sci. Technol.* **10**, 523-542 (1997).
- [19] E. Lengyel, M. Nicklas, H. S. Jeevan, C. Geibel, and F. Steglich, *Phys. Rev. Lett.* **107**, 057001 (2011).
- [20] M. Bendele, A. Amato, K. Conder, M. Elender, H. Keller, H.-H. Klauss, H. Luetkens, E. Pomjakushina, A. Raselli, and R. Khasanov, *Phys. Rev. Lett.* **104**, 087003 (2010).
- [21] D. M. Hawley and G. Ferguson, *J. Chem. Soc. (A)* 2059-2063 (1968).
- [22] P. G. Jones, A. Blaschette, D. Henschel, and A. Weitze, *Zeitschrift für Kristallographie* **210**, 377-378 (1995).
- [23] C. W. Glass, A. R. Oganov, and N. Hansen, *Comp. Phys. Comm.* **175**, 713-720 (2006).
- [24] G. Kresse and J. Hafner, *Phys. Rev. B* **47**, 558-561 (1993).
- [25] G. Kresse and J. Furthmüller, *Phys. Rev. B* **54**, 11169-11186 (1996).
- [26] J. P. Perdew, K. Burke, and M. Ernzerhof, *Phys. Rev. Lett.* **77**, 3865-3868 (1996).
- [27] P. E. Blöchl, *Phys. Rev. B* **50**, 17953-17979 (1994).
- [28] C. Ludwig and H.-J. Götze, *Spectrochimica Acta Part A* **51**, 2019-2026 (1995).
- [29] K. Shobatake, C. Postmus, J. R. Ferraro, and K. Nakamoto, *Applied Spectroscopy* **23**, 12-16 (1969).
- [30] D. H. Whiffen, *J. Chem. Soc.* 1350-1356 (1956).